Thermodynamic Determination of the Na^+:Glucose Coupling Ratio for the Human SGLT1 Cotransporter

Xing-Zhen Chen,* Michael J. Coady,‡ Francis Jackson,* Alfred Berteloot,‡ and Jean-Yves Lapointe*
Groupe de recherche en transport membranaire, *Département de Physique, and ‡Département de Physiologie, Université de Montréal, Montréal, Québec H3C 3J7, Canada

ABSTRACT Phlorizin-sensitive currents mediated by a Na-glucose cotransporter were measured using intact or internally perfused *Xenopus laevis* oocytes expressing human SGLT1 cDNA. Using a two-microelectrode voltage clamp technique, measured reversal potentials (V_r) at high external α-methylglucose (αMG) concentrations were linearly related to $\ln[\alpha MG]_o$, and the observed slope of 26.1 ± 0.8 mV/decade indicated a coupling ratio of 2.25 ± 0.07 Na ions per αMG molecule. As $[\alpha MG]_o$ decreased below 0.1 mM, V_r was no longer a linear function of $\ln[\alpha MG]_o$, in accordance with the suggested capacity of SGLT1 to carry Na in the absence of sugar (the "Na leak"). A generalized kinetic model for SGLT1 transport introduces a new parameter, K_c, which corresponds to the $[\alpha MG]_o$ at which the Na leak is equal in magnitude to the coupled Na-αMG flux. Using this kinetic model, the curve of V_r as a function of $\ln[\alpha MG]_o$ could be fitted over the entire range of $[\alpha MG]_o$ if K_c is adjusted to 40 ± 12 μM. Experiments using internally perfused oocytes revealed a number of previously unknown facets of SGLT1 transport. In the bilateral absence of αMG, the phlorizin-sensitive Na leak demonstrated a strong inward rectification. The affinity of αMG for its internal site was low; the K_m was estimated to be between 25 and 50 mM, an order of magnitude higher than that found for the extracellular site. Furthermore, V_r determinations at varying αMG concentrations indicate a transport stoichiometry of 2 Na ions per αMG molecule: the slope of V_r versus $\ln[\alpha MG]_o$ averaged 30.0 ± 0.7 mV/decade (corresponding to a stoichiometry of 1.96 ± 0.04 Na ions per αMG molecule) whenever $[\alpha MG]_o$ was higher than 0.1 mM. These direct observations firmly establish that Na ions can utilize the SGLT1 protein to cross the membrane either alone or in a coupled manner with a stoichiometry of 2 Na ions per sugar molecule.

INTRODUCTION

Sodium-glucose cotransporters are present in the brush border membranes of renal proximal tubule and small intestinal villous cells and are directly involved in transepithelial glucose reabsorption. Despite the numerous studies carried out over the past two decades and summarized in several reviews (Crane et al., 1977; Semenza et al., 1984; Kimmich, 1990; Silverman, 1991; Wright, 1993), nothing is known concerning the molecular mechanism by which the two substrates are coupled, and the choice of kinetic model remains a matter of debate (Kessler and Semenza, 1983; Restrepo and Kimmich, 1985; Parent et al., 1992b). There are known to be at least two Na^+-glucose cotransporter genes (Scriver and Tenenhouse, 1985; Mackenzie et al., 1994), and the simultaneous presence in renal tissue of two different transporters with similar activities has further confounded the study of Na-glucose cotransport kinetics.

One aspect of kinetic models that has been much investigated is the stoichiometric ratio between the two transported substrates. Studies of the coupling of Na and glucose have generally employed the measurement of radiolabeled substrate uptake into membrane vesicles or intact cells. Using this approach, Kimmich's laboratory recognized (Kimmich and Randles, 1980, 1984) that many attempts to determine the stoichiometric ratio were affected by an inadequate control of the membrane potential. When efforts were made to clamp membrane potential, the estimated stoichiometric ratio changed from 1:1 to a value closer to 2:1 in chicken enterocytes as determined by comparing sugar-induced Na fluxes to Na-induced sugar fluxes (n = 1.7–1.9; Kimmich and Randles, 1984). Also, sigmoidicity in the dependence of Na-glucose cotransport on external Na in late proximal tubules (Turner and Moran, 1982b) and in a cultured renal cell line (Moran et al., 1982; Lever, 1982) suggested that two Na ions were required for the cotransport of each glucose molecule. Similar experiments performed in the S1 segment of proximal convoluted tubules (Turner and Moran, 1982a) indicated that only one Na ion was required per glucose molecule in this segment. However, such sigmoidicity is related to the number and affinities of Na ions reacting with the transporter and not necessarily to the number of Na ions that are cotransported. Two methods of accurately measuring the true stoichiometric ratio for cotransported substrates exist: i) balancing the Na concentration gradient with an opposed glucose concentration gradient (static head method) or ii) finding the zero current potential for the cotransport (reversal potential determination). Based on such thermodynamic approaches, it was concluded that one Na ion was actually transported per sugar molecule in *Necturus* small intestine (Lapointe et al., 1986) and in early proximal tubules (Turner and Moran, 1982a), whereas in late proximal tubules a stoichiometry of 2:1 was suggested (Turner and Moran, 1982b). More re-

Received for publication 16 May 1995 and in final form 6 September 1995.
Address reprint requests to Dr. Jean-Yves Lapointe, Groupe de recherche en transport membranaire, Département de Physique, Université de Montréal, C.P. 6128, succursale centre-ville, Montréal, Québec H3C 3J7, Canada. Tel: 514-343-7046; Fax: 514-343-2111; E-mail: lapoinj@ere.umontreal.ca.

0006-3495/95/12/2405/10 $2.00

cently, reversal potentials for Na-glucose cotransport were determined for LLC-PK_1 cells under whole-cell voltage clamp conditions (Smith-Maxwell et al., 1990). Although the measured values were consistent with a stoichiometric ratio of two Na ions to one glucose molecule, the precision of the data did not permit an unambiguous differentiation between a 2:1 and a 1:1 coupling ratio.

Investigation into sodium-glucose cotransport was reoriented by the cloning of the cDNA for the rabbit sodium-glucose cotransporter (SGLT1) in 1987 (Hediger et al., 1987). This protein has been characterized in some detail using mRNA-injected *Xenopus laevis* oocytes (Parent et al., 1992a,b; Loo et al., 1993; Wright, 1993), permitting a high level of SGLT1 expression in the effective absence of other Na^+-glucose cotransporters. The Na:glucose coupling stoichiometry for the cloned transporter was deduced as 2:1 either on the basis of transport sigmoidicity with varying extracellular Na concentration ($[Na]_O$) (Parent et al., 1992a, Hill number = 1.9; Wright, 1993, Hill number = 1.6) or by a direct comparison between Na current (in voltage clamp conditions) and sugar uptake (n = 1.8 in Lee et al., 1994 and n = 1.44 in Mackenzie et al., 1995). The limitations of using sigmoidicity in the former procedure to estimate stoichiometric ratios have been outlined above; those of the latter procedure will be considered in the discussion. Further complicating the relationship between the Na and glucose transport of SGLT1, Umbach et al. (1990) have shown that a phlorizin (pz)-sensitive current through SGLT1 persisted even in the absence of external glucose. They concluded that this current, which was dependent on $[Na]_O$, was a Na leak, which suggested that a strict coupling between Na and glucose fluxes could be broken at low extracellular glucose concentrations.

In this study, we will present direct experimental support for a 2 Na:1 glucose stoichiometry for human SGLT1-mediated cotransport using both a two-microelectrode voltage clamp technique and the cut-open oocyte technique, which ensures the control of membrane potential as well as of intracellular Na and sugar concentrations. In addition, the current-voltage (I-V) relationship of the inwardly rectifying Na leak will be presented together with a numerical simulation showing the relative Na fluxes by the Na leak and by the Na-glucose cotransport at different extracellular sugar concentrations. This permits further clarification of the kinetic mechanism by which SGLT1 operates.

MATERIALS AND METHODS

Oocyte preparation and injection

Stage V or VI oocytes were removed from *Xenopus laevis* frogs anesthetized with 3-aminobenzoic acid ethyl ester. The follicular layer was removed by incubation in Barth's solution containing 2–3 U/ml collagenase (Boehringer Mannheim, Laval, QC) for 1 to 2 h, followed by agitation of the oocytes in a Ca^{2+}-free Barth's solution for 45 min. The composition of Barth's solution is 88 mM NaCl, 3 mM KCl, 0.82 mM $MgSO_4$, 0.41 mM $CaCl_2$, 0.33 mM $Ca(NO_3)_2$ and 5 mM HEPES, pH 7.60. Defolliculated oocytes were stored at 18°C in Barth's solution containing 5% horse serum, 2.5 mM Na pyruvate, 100 U/ml penicilin, and 0.1 mg/ml streptomycin (referred to henceforth as antibiotic Barth's solution). A full-length human SGLT1 cDNA was obtained using PCR on human jejunal cDNA based on published sequence data (Hediger et al., 1989). The primers used were AATTCCGCTGCCACCATGGACAGT and TCGAGGAGGACGGACAGGAAAAGTG, and correspond primarily to untranslated regions of the cDNA (base pairs 1–19 and 2391–2413). The primers were phosphorylated before use, and PCR amplification was performed using Pfu polymerase (Stratagene, San Diego, CA) with one cycle of 5′ at 95°C, 5′ at 54°C, and 7′ at 75°C followed by 29 cycles of 2′ at 95°C, 1′ at 54°C, and 7′ at 75°C. The 2.4-kb PCR product was then treated with Exonuclease III (Kaluz et al., 1992) and inserted into the vector pMT21 (kindly provided by the Genetics Institute, Boston, MA), which had been cut with *Eco*RI and *Xho*I. This construct was used for injection into *Xenopus* oocyte nuclei (Swick et al., 1992). The nuclear injection of 270 pg of recombinant pMT21-SGLT1 together with 30 pg of a similar construct coding for secreted expressed alkaline phosphatase (Swick et al., 1992) was performed 1 day after obtaining defolliculated oocytes. The injected oocytes were incubated in antibiotic Barth's solution supplemented with 100 μM phlorizin for 24 to 36 h before incubating individual oocytes in Barth's solution deprived of serum (200 μl solution for each oocyte) for another 24 to 36 h. Then 100 μl of incubation solution from each oocyte was mixed with 140 μl of alkaline phosphatase assay solution as described by Tate et al. (1990) and held at 40°C for 2 to 10 h. The oocytes expressing alkaline phosphatase were selected by visual inspection of the colorimetric alkaline phosphatase reaction. In general, 10% to 25% of injected oocytes were found to be positive for alkaline phophatase expression, and all expressed SGLT1. α-Methylglucose (αMG) and phlorizin were used as a specific substrate and inhibitor for SGLT1, respectively.

Two-microelectrode voltage clamp technique

Solutions used for the two-microelectrode voltage clamp technique contained 70 mM NaCl, 3 mM KCl, 0.82 mM $MgSO_4$, 0.41 mM $CaCl_2$, 0.33 mM $Ca(NO_3)_2$, 5 mM HEPES, pH 7.60, and 40 mM (mannitol + αMG). Currents through the SGLT1 cotransporter were determined as the difference between currents measured before and after the addition of phlorizin. The two-microelectrode voltage clamp technique used in the present study has been described in recent papers from this laboratory (Coady et al., 1994; Huang et al., 1995). In noninjected or water-injected oocytes, addition of 5 mM αMG generated a negligibly small current (~5 nA at −50 mV), which was not subtracted from current measurements in SGLT1-expressing oocytes (300–1000 nA at −50 mV). No phlorizin-sensitive currents were observed (<2–5 nA) using control oocytes in the absence of αMG.

Cut-open oocyte technique

The cut-open oocyte technique consists of electrically isolating a membrane patch (with a diameter of 0.65 mm) representing approximately 8% of the total membrane surface, through which membrane currents can be measured while the intracellular face of the membrane is continuously perfused. Several modifications of the original version of Taglialatela et al. (1992) were implemented, some of which have been described by Costa et al. (1994). We used a low-access resistance (about 200 kΩ) glass pipette to perfuse the intracellular space and to measure membrane potential (Fig. 1), without puncturing the membrane patch, as with conventional microelectrodes. Another modification made to the original design was that a high flow rate (5–8 μl/min) was used to perfuse the cytosolic face of the oocyte. To allow rapid pipette solution exchange, the input flow rate was set to 40–43 μl/min using a hydrostatic pressure of 70 cm H_2O and a high hydraulic resistance in the line to stabilize the flow rate. The drain flow rate was set to 35 μl/min using a similar hydrostatic pressure drain system. Finally, the upper compartment and the guard compartment were both clamped to 0 mV using a custom-made amplifier. When the interior of the oocyte was pulsed to different potentials, the current recorded from the

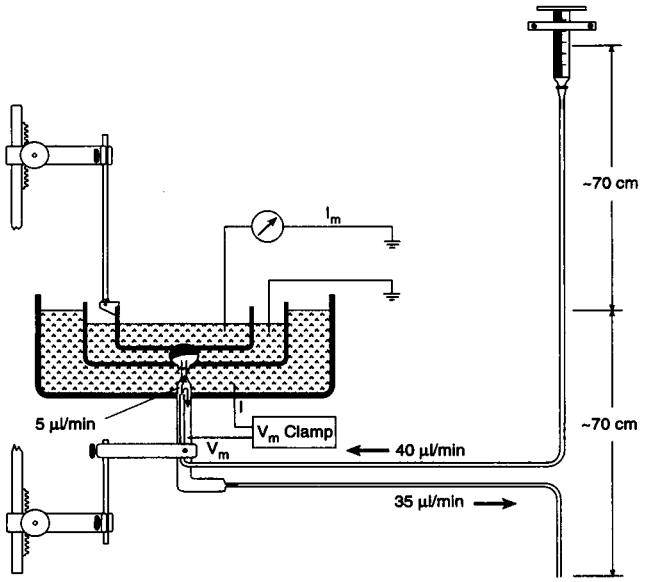

FIGURE 1 Schematic representation of the experimental set-up used for the cut-open oocyte technique. It consists of physically and electrically isolating a membrane patch through which membrane current is measured while a glass pipette is used to measure the intracellular potential and perfuse the intracellular space.

upper compartment must have originated from within the isolated membrane patch. The extracellular solution used with the cut-open oocyte technique consisted of 43.8 mM Na cyclamate, 6.2 mM NaCl, 1 mM $MgCl_2$, 0.9 mM $CaCl_2$, 5 mM HEPES, pH 7.6, 80 mM (mannitol + αMG), and 3 mM *N*-methyl-D-glucamine. The intracellular perfusion solution differed from the extracellular solution only in that it contained 75 mM (mannitol + αMG), 1 mM EGTA, and 6 mM *N*-methyl-D-glucamine.

The generation of voltage pulses and data acquisition as well as the storage and analysis of data were performed using the Pclamp Program (Version 5.5.1, Axon Instruments, Foster City, CA).

Theoretical expressions for the reversal potential in the presence of a Na leak

For any given transport process occurring through a well-defined stoichiometry, equilibrium will be reached when the Gibbs free energy remains constant after one transport cycle, i.e., when

$$dG = \sum_i \mu_i \, dn_i = 0, \qquad (1)$$

where μ_i is the electrochemical potential of each transported molecule and dn_i is the number of molecules transported per cycle (Schultz, 1980). In the case of Na-glucose cotransport, using the expression for the electrochemical potential for Na and glucose (where G represents the sugar substrates for SGLT1) on each side of the membrane and solving for the zero current potential (V_r, called a reversal potential or equilibrium potential in this case), the following expression is derived:

$$V_r = \frac{RT}{nF} \ln \frac{[G]_o[Na]_o^n}{[G]_i[Na]_i^n}, \qquad (2)$$

where $[Na]_o$ or $[Na]_i$ ($[G]_o$ or $[G]_i$) is Na (glucose) concentration outside or inside the oocyte, n is the number of Na ions transported per glucose molecule, and R, T, and F have their usual meanings. If it is assumed that $[G]_i$, $[Na]_i$, and $[Na]_o$ remain constant, a linear relationship is found between V_r and $\ln[G]_o$:

$$V_r = (25.4/n \text{ mV})\ln[G]_o + C \quad (\text{at } 22°C) \qquad (3)$$

where C is a constant.

The presence of a putative Na leak complicates the relationship between V_r and substrate concentrations. To describe V_r in the presence of both coupled Na-glucose transport and a Na leak, we considered a symmetrical kinetic model where an arbitrary number of steps from free enzyme to the complex with n Na ions bound is allowed (Fig. 2 *A*). The expression for V_r is given by (see Appendix)

$$V_r = \frac{RT}{nF} \ln \frac{([G]_o + K_c)[Na]_o^n}{([G]_i + K_c)[Na]_i^n}. \qquad (4)$$

If $[G]_i$, $[Na]_i$, and $[Na]_o$ are assumed constant, then

$$V_r = (25.4/n \text{ mV})\ln([G]_o + K_c) + D, \qquad (5)$$

where D is a constant. K_c is a characteristic concentration constant whose derivation is described in the Appendix; it represents the glucose concentration at which the Na leak is equal to the Na flux coupled to glucose

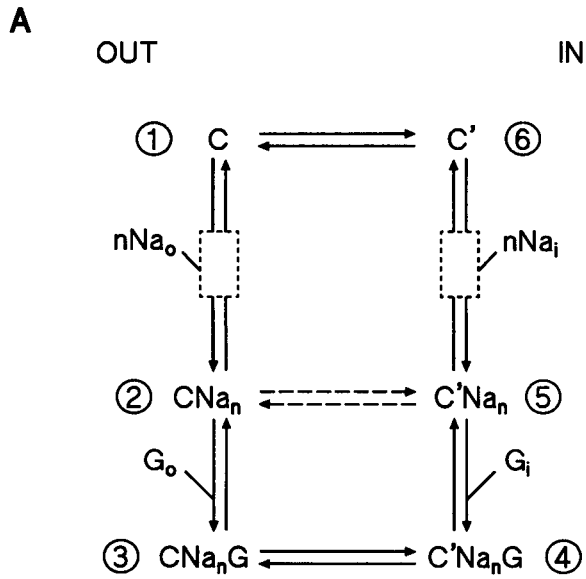

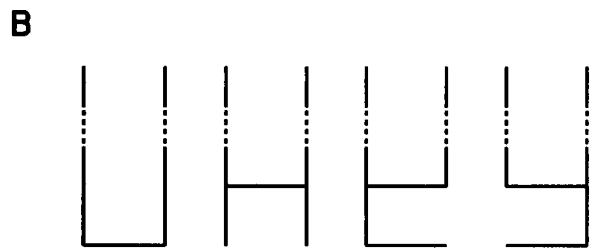

FIGURE 2 (*A*) Generalized symmetrical kinetic model. At each side of the membrane, the binding of n Na ions is described by an arbitrary number of steps (inside the box) between the free carrier state C (or C′) and the complex CNa_n (or $C'Na_n$). (*B*) The complete set of King-Altman graphics (King and Altman, 1956) contributing to the transmembrane current.

transport. Note that Eq. 4 becomes Eq. 2 if no Na leak ($K_c = 0$) is present or, alternatively, if both $[G]_o$ and $[G]_i \gg K_c$.

Statistical analysis

Experimental results were expressed in the form of mean ± SEM (N), where N indicates the number of oocytes obtained from at least two different donors. Paired or unpaired Student's t-test was used to compare two sets of data whenever appropriate. The curve-fitting procedures were performed with equal weighting using commercially available software (FigP v. 6.0, Elsevier-Biosoft, Cambridge, England).

RESULTS

Intact oocytes

Fig. 3 *A* shows the oocyte currents recorded at a membrane potential of −50 mV when 50 μM phlorizin or different concentrations of αMG were added to the bath. The slow response of membrane currents observed when αMG replaced phlorizin is due to the fact that phlorizin binds to the transporter immediately (as fast as our external solution exchange speed allows, i.e., 5–10 s) but remains bound to the transporter for several tens of seconds after complete removal of external phlorizin, as previously reported (Restrepo and Kimmich, 1986). The differences between currents measured before and after phlorizin addition for the three $[\alpha MG]_o$ shown in Fig. 3 *A* are illustrated in Fig. 3 *C*. When similar experiments were done using 70 mM Na_o and a variety of $[\alpha MG]_o$, average $K_m^{\alpha MG}$ values of 1.3 ± 0.2 mM and 0.8 ± 0.1 mM ($N = 5$) were found at, respectively, −50 mV and −100 mV. For each *I-V* curve of the type shown in Fig. 3 *C*, it is possible to determine a reversal potential (V_r); these are plotted against $\ln[\alpha MG]_o$ in Fig. 4. Note that a V_r corresponding to $[\alpha MG]_o = 0$ mM could be measured; at −100 mV, this putative Na leak under zero $[\alpha MG]_o$ conditions averaged 28.9 ± 5.0 nA ($N = 4$), corresponding to 2.5% of the maximal cotransport current. The V_r at zero $[\alpha MG]_o$ is not predicted by Eq. 3, which fit these data only for $[\alpha MG]_o > 0.1$ mM (*dashed line*). The entire data set can be well fit, however, using Eq. 5 with parameters "n" (stoichiometry) and K_c (Fig. 4, *solid line*) as described in the figure legend. The improved fit gave an n value of 2.25 ± 0.07 ($N = 6$) (or a mean slope of 26.1 ± 0.8 mV/decade) and, in the cases where currents at low $[\alpha MG]_o$ could be accurately measured, an averaged value for K_c of 40 ± 12 μM ($N = 3$) was found. This analysis is based on the assumption that internal sodium and glucose concentrations remain unchanged during the experiment. Because of doubts regarding this assumption, we continued our experiments by using internally perfused oocytes, which permit control of the cytosolic environment.

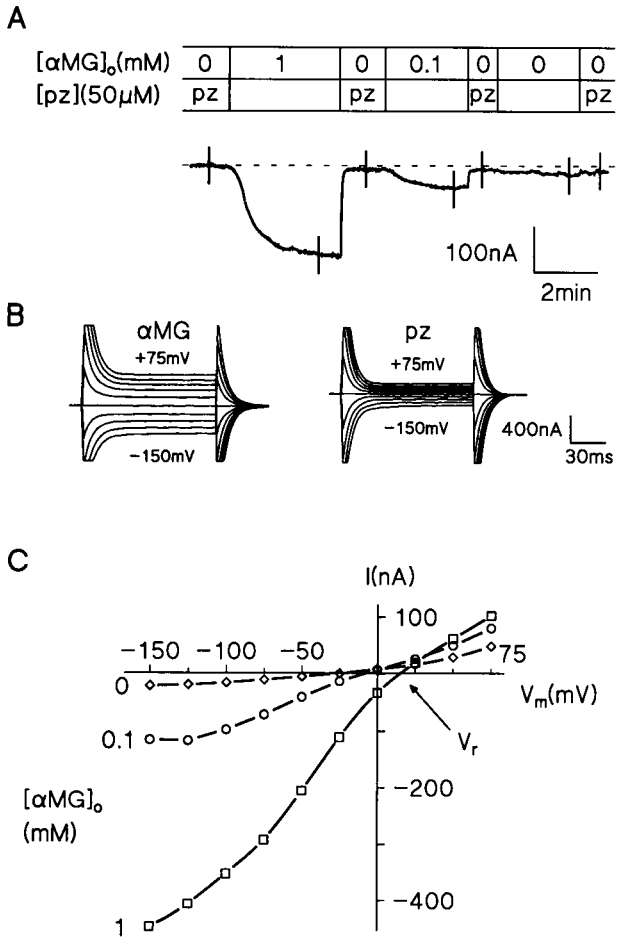

FIGURE 3 SGLT1 current measurements using a two-microeletrode voltage clamp technique. (*A*) Recording of membrane currents at a membrane potential (V_m) of −50 mV. A series of voltage pulses was applied at each vertical line shown in the current record, to generate *I-V* curves. (*B*) Examples of measured membrane currents in the presence of 1 mM αMG_o or 50 μM pz, from data recording shown in part *A*. (*C*) *I-V* curves for pz-sensitive currents at different $[\alpha MG]_o$ were obtained as the differences between currents measured before and after a 50 μM phlorizin application. Reversal potentials (V_r) are interpolated as zero current potentials.

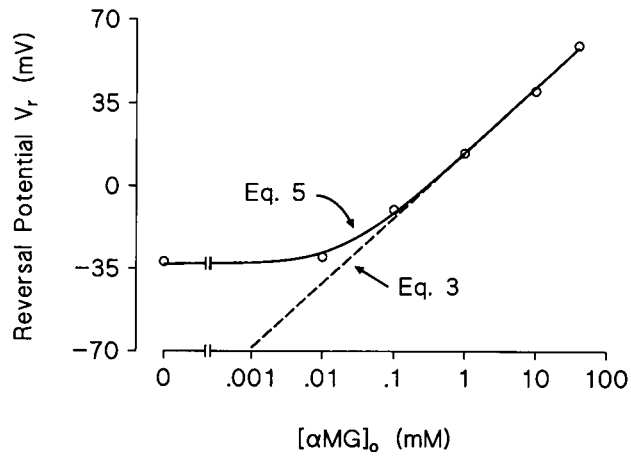

FIGURE 4 Nonlinearity between SGLT1 reversal potentials and $\ln[\alpha MG]_o$. Data points show reversal potentials (V_r) determined for different $[\alpha MG]_o$ in a typical experiment of the type shown in Fig. 3. The straight line is a best fit using a formula based on simple thermodynamic considerations (Eq. 3). The curved line is an improved fit using the formula (Eq. 5) derived from the generalized kinetic model (see Appendix), which introduces a characteristic concentration constant (K_c). Assuming that $[Na]_i$ and $[\alpha MG]_i$ are constant, values of $n = 2.11$ and $K_c = 20$ μM were obtained in this example.

Internally perfused oocytes

Fig. 5 *A* shows the effect of external αMG addition on the membrane current recorded from a patch of membrane while the oocyte was internally perfused with 0 mM αMG and 50 mM Na at −60 mV. Phlorizin-sensitive currents (Fig. 5 *C*) were determined from two consecutive *I-V* curves generally done within 20 s of each other. The external $K_m^{\alpha MG}$ showed no dependence on membrane potential from −160 mV to −60 mV and averaged 3.4 ± 0.5 mM ($N = 7$). This value is larger than that measured in intact oocyte experiments, possibly because the intracellular Na concentration ($[Na]_i$ = 50 mM) used in cut-open oocyte experiments is much higher than the $[Na]_i$ of intact oocytes (7–20 mM, Lafaire and Schwartz, 1986; 6–22 mM, Dascal, 1987). Higher $[Na]_i$ is expected to increase the external K_m^G values, as discussed by Kessler and Semenza (1983) for brush border membrane vesicle uptake experiments. An αMG_i-induced outward current (in the absence of αMG_o) at a holding potential (V_h) of −20 mV is shown in Fig. 6. One can see that, using our fast perfusion rate, a steady-state current is reached within 2 min after the application of a new internal solution. As shown in Fig. 6, it is clear that the affinity of the internal site for αMG is very low inasmuch as 37.5 mM αMG did not saturate the SGLT1 internal binding site for sugar. In three independent experiments where several $[\alpha MG]_i$ could be tested sequentially on the same oocyte, the internal $K_m^{\alpha MG}$ was estimated to be between 25 and 50 mM. Reversal potentials were measured in four independent experiments under zero $[\alpha MG]_o$ condition, with different $[\alpha MG]_i$; an average K_c of 28 ± 5 μM was obtained using Eq. 5. This K_c value is close to that obtained with intact oocytes.

The phlorizin-sensitive current in the absence of αMG on either side of the membrane (the putative Na leak) was also measurable using cut-open oocytes. Both extracellular and intracellular perfusates contained 50 mM Na, and the pz-sensitive current was shown to possess strong inward rectification (see Fig. 7 for average currents from five oocytes). Note that the average outward current of 1.7 ± 0.8 nA at 0 mV is not statistically different from zero.

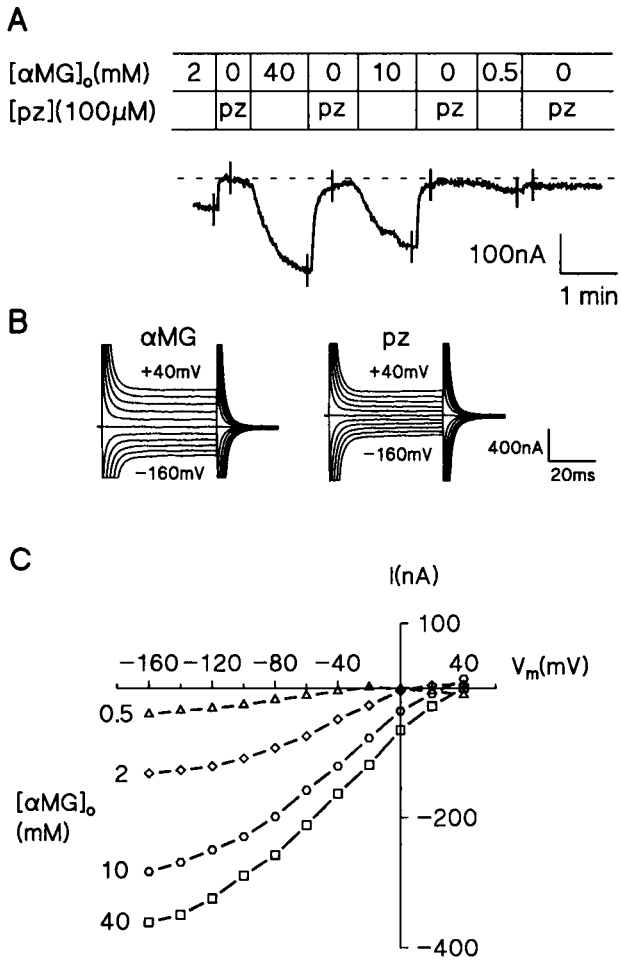

FIGURE 5 SGLT1 current measurements using the cut-open oocyte technique. (*A*) Recording of membrane currents at a membrane potential (V_m) of −60 mV. (*B*) Examples of measured membrane currents upon applying a series of voltage pulses in the presence of 10 mM αMG_o or 100 μM pz. (*C*) *I-V* curves for pz-sensitive currents at different $[\alpha MG]_o$ were obtained as the differences between currents measured before and after a 100 μM phlorizin application.

SGLT1 stoichiometry in internally perfused oocytes

With internally perfused oocytes, a single determinaton of V_r can be used to obtain the stoichiometric parameter "*n*" from Eq. 2, provided that $[\alpha MG]_o$ and $[\alpha MG]_i$ are large enough that the Na leak becomes effectively negligible. An example with $[\alpha MG]_i$ = 30 mM and $[\alpha MG]_o$ = 2 mM is shown in Fig. 8 *A* where both the theoretical V_r position corresponding to $n = 2$ and the measured V_r position (n = 1.96) are indicated. We see that the measured V_r was within 1 mV of the theoretical value for $n = 2$. To increase

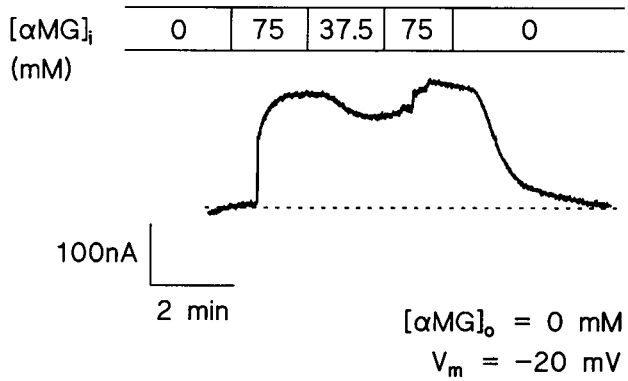

FIGURE 6 Measurement of αMG_i-induced currents in cut-open oocytes. Current began to change 30 s after a new solution was perfused internally. This period is the time necessary to replace the previous solution in the line feeding the oocyte perfusion system. The current then reaches a plateau within 2 min. αMG_i-induced currents were reversible when substrate concentration was repeatedly raised or lowered.

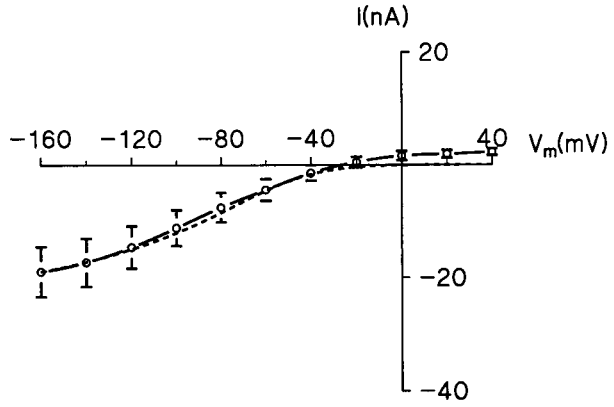

FIGURE 7 Inward rectification of the Na leak. An inwardly rectifying Na current, i.e., pz-sensitive current in the complete absence of sugar on either side of the membrane, was observed in all oocytes expressing SGLT1. Data points represent the average result from five oocytes. The dashed line represents a numerical simulation fitting these data points (see text). $[Na]_i = [Na]_o = 50$ mM, [Pz] = 100 μM.

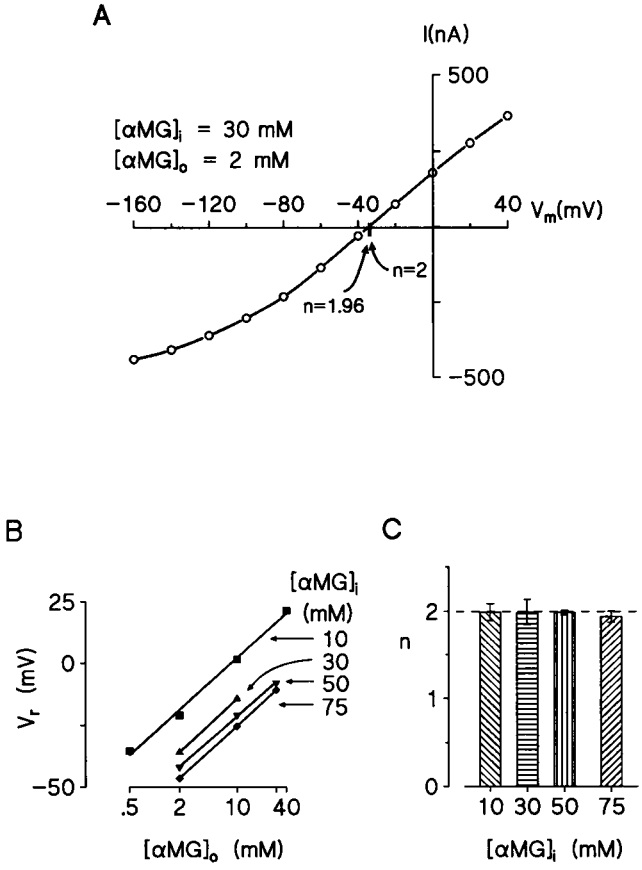

FIGURE 8 Determination of SGLT1 stoichiometry ("n") using cut-open oocytes. (*A*) Example of phlorizin-sensitive current-voltage relationship using perfusion of both membrane faces with known αMG concentrations. $[Na]_i = [Na]_o = 50$ mM. The vertical lines show the reversal potentials for the measured value of n (1.96) as well as for the theoretical value of 2. (*B*) V_r was plotted as a function of $[\alpha MG]_o$ using different intracellular αMG concentrations from 10 to 75 mM. To improve accuracy, the stoichiometric ratio "n" is determined from the slope of each line, which equals 58.5/n mV decade at 22°C. (C) The "n" values determined from different experiments using internal αMG concentrations up to 75 mM do not differ significantly from 2. The "n" value at 10 mM αMG_i was obtained from three experiments; the values at 30, 50, and 75 mM αMG_i are from three, two, and ten experiments, respectively.

accuracy and to make the stoichiometric determination completely independent from any offset in the absolute values of V_m, V_r was measured at several $[\alpha MG]_o$ and the slope of the V_r versus $\ln[\alpha MG]_o$ relationship was used. As shown in Fig. 8 *B*, this determination was repeated at different $[\alpha MG]_i$, yielding lines of almost identical slopes. The stoichiometry parameter "n" turned out to be independent of $[\alpha MG]_i$ from 10 mM to 75 mM (see Fig. 8 *C*) or of $[\alpha MG]_o$ from 0.5 to 40 mM, and an average value of 1.96 $\pm$ 0.04 was obtained from the pooled data (N = 18 determinations), which is not significantly different from 2.

DISCUSSION

SGLT1 was among the first membrane cotransporters to be cloned, and its transport mechanism has been studied in detail using steady-state and pre-steady-state electrophysiological methods (Umbach et al., 1990; Parent et al., 1992a,b; Loo et al., 1993; Wright, 1993). In these and earlier studies, the proposed stoichiometry of two Na ions per glucose molecule has relied almost exclusively on the sigmoidal activation curve by extracellular Na with a Hill number ranging from 1.6 to 1.9 (Wright, 1993; Parent et al., 1992a; Turner and Moran, 1982b; Moran et al., 1982). We felt that this question could be better addressed by employing a conventional two-microelectrode voltage clamp technique on intact oocytes as well as the cut-open oocyte technique, to examine reversal potentials of SGLT1-specific *I-V* curves. The results presented above indicate that SGLT1 definitely cotransports two Na ions per glucose molecule when the αMG concentration is much larger than a newly defined characteristic concentration K_c (~40 μM). At low $[\alpha MG]_o$, the uncoupled Na flux represents a substantial part of Na transport through SGLT1.

Stoichiometry of two Na ions per glucose molecule

Using the two-microelectrode voltage clamp technique, V_r was shown to vary linearly with $\ln[\alpha MG]_o$ as long as $[\alpha MG]_o$ remains higher than 0.1 mM. The slope of this line is consistent with a stoichiometry of two Na ions transported per αMG molecule. The measured "n" value is, in fact, slightly (but significantly) larger than 2, which suggests that our assumption of intracellular Na and sugar concentrations remaining constant during the experiment is not sufficiently accurate. If intracellular αMG concentrations increase with $[\alpha MG]_o$, the gradient of αMG will be less than presumed and V_r will change less than predicted. This leads to a lower slope in the V_r versus $\ln[\alpha MG]_o$ curve and thus a larger calculated value of "n." This hypothesis is

supported by the fact that higher $[\alpha MG]_o$ give larger outward currents at positive potentials (Fig. 3 *C*). As the Na leak cannot explain outward currents of this magnitude (the Na leak is strongly inward rectifying; see Fig. 7), these currents are most likely due to some significant sugar accumulation in the immediate vicinity of the intracellular face of the membrane during exposure to αMG_o.

When oocytes were perfused with sugar-free solutions using the cut-open oocyte technique, very small outward currents were detected at positive membrane potentials (see Figs. 5 *C* and 7), indicating efficient control of the intracellular solution. In the presence of $[\alpha MG]_i$, the absolute values of the reversal potential measured were always consistent with a coupling stoichiometry of two Na ions per αMG molecule. A more accurate way to obtain "*n*" is to consider the variation of V_r as a function of $\ln[\alpha MG]_o$; this eliminates the influence on "*n*" of any offset (even of a few millivolts) in the voltage measurement circuit. The coupling stoichiometry using this thermodynamical approach was found to be 1.96 ± 0.04 ($N = 18$), a value not significantly different from two Na ions per αMG molecule (Fig. 8 *C*). This parameter was found to be independent of $[\alpha MG]_i$ over the entire range covered (10–75 mM).

Recently, lower values of "*n*" were reported for SGLT1 expressed in oocytes ($n = 1.8$ in Lee et al., 1994 and $n = 1.44$ in Mackenzie et al., 1995). The coupling stoichiometry was obtained by comparing the net Na flux through SGLT1 (estimated from the phlorizin-sensitive current) to the unidirectional αMG uptake under similar or identical conditions. Although it is clear that the stoichiometric ratio for SGLT1 can be obtained by comparing the ratio of net fluxes of the two substrates, the assumption that unidirectional αMG uptake is equal to the net sugar flux depends on experimental conditions. There can be an exchange of radiolabeled external sugar for intracellular sugars without dissociation of Na ions from the carrier, which would result in artifactually low stoichiometric ratios. Although the level of intracellular glucose in *Xenopus laevis* oocytes has been reported to be below 50 μM (Umbach et al., 1990), the outward phlorizin-sensitive currents observed by us and others (present study; Umbach et al., 1990) indicates the intracellular presence of some forms of SGLT1 substrates. These currents, which can be observed before the first external sugar exposure, reverse between -20 and -45 mV and cannot be solely accounted for by a Na leak. Hence, the assumption that unidirectional tracer uptake is representative of net sugar flux appears to be inaccurate.

Na leak

We have seen (Fig. 4) that the straightforward thermodynamic expression for V_r (Eq. 3) failed to fit the relationship between V_r and $\ln[\alpha MG]_o$ for $[\alpha MG]_o < 0.1$ mM. The generalized kinetic model (Fig. 2 *A*), which allows *n* Na ions to cross the membrane without sugar cotransport, gives a slightly different formula for this relationship (Eq. 5) and introduces a characteristic concentration constant K_c. This K_c can easily be obtained from fitting experimental data to Eq. 5. As described in the Appendix, K_c represents the sugar concentration at which the Na leak is equal to Na-sugar cotransport. In the complete absence of αMG (on both sides) an inwardly rectifying Na leak was obtained (Fig. 7), which indicates both that the cytoplasmic face of the membrane is adequately perfused, and that a large asymmetry exists between the forward and reverse reactions of some rate-limiting steps. In this case, a four-state kinetic model (equivalent to the upper cycle of the six-state model in Loo et al., 1993) can be used to describe the Na leak behavior. Rate constants describing Na binding to (k^0_{12}) and debinding from (k^0_{21}) the extracellular site and the constants for free carrier conformational changes (k^0_{16} and k^0_{61}) were taken from Loo et al. (1993). Rate constants k^0_{25} and k^0_{52}, directly related to the Na leak, were adjusted to fit the *I-V* curve of the Na leak (dashed line in Fig. 7). The optimal values are shown in Fig. 9 *A*. The fit at positive potentials can be significantly improved if the original rate constants from Loo et al. (1993) are changed as follows: k^0_{12} from 14,000 to 40,000 $s^{-1}mole^{-2}$, k^0_{61} from 25 to 50 s^{-1}, and k^0_{21} from 300 to 150 s^{-1}. This set of parameters remains consistent with the pre-steady-state data reported by Loo et al. (1993).

Kinetic parameters for human SGLT1

Based on the rate constants given above, quantitative values can be proposed for a six-state kinetic model of the human SGLT1 that incorporates the new parameters provided in the present study (K_c, and both external and internal $K_m^{\alpha MG}$) and that is similar to that originally proposed by Parent et al. (1992b) for the rabbit cotransporter. We have chosen this model rather than others (Kimmich, 1990; Silverman, 1991; Stevens, 1992) because it is simple and consistent with an extensive set of data obtained in SGLT1-expressing oocytes, including pre-steady-state currents and the observed Na leak. k^0_{23} and k^0_{45} values were derived from the external and internal $K_m^{\alpha MG}$; k^0_{65} and k^0_{54} were calculated using two microscopic reversibility relations; and k^0_{34}, k^0_{43}, k^0_{32}, and k^0_{56} were adopted from Parent et al. (1992b). The proposed kinetic parameters are given in Fig. 9 *A*. This kinetic model can help in predicting the proportions between the two transport modes studied in the present paper: $J_{3\to4}$, representing the coupled Na-glucose influx, and $J_{2\to5}$, representing the inward Na leak. These quantities were calculated as a function of $[\alpha MG]_o$ and are presented in Fig. 9 *B*. We see that, as $[\alpha MG]_o$ increases, the coupled Na-αMG influx ($J_{3\to4}$) increases and the inward Na leak ($J_{2\to5}$) decreases toward zero, and that $J_{2\to5}$ is equal to $J_{3\to4}$ at K_c (32 μM, consistent with the measured values of 40 ± 12 μM in intact oocytes and 28 ± 5 μM in internally perfused oocytes). As expected (see Appendix), the ratio $J_{3\to4}/J_{2\to5}$ comprises a straight line equal to $[\alpha MG]_o/K_c$ from which the relative magnitudes

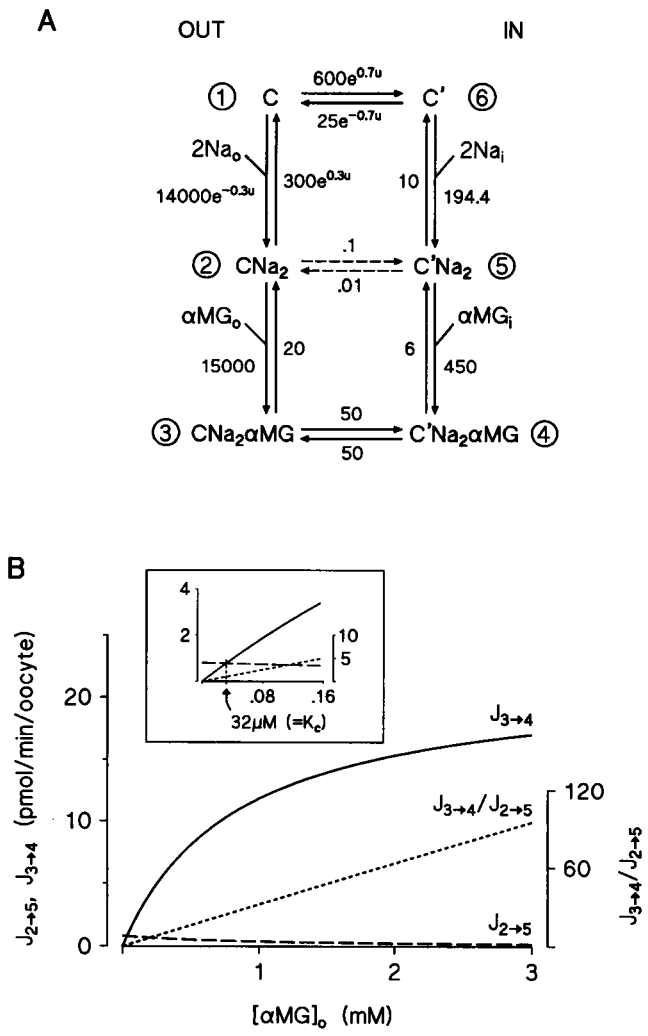

FIGURE 9 Numerical modeling of Na currents. (*A*) A symmetrical ordered six-state kinetic model for human SGLT1, originally proposed by Parent et al. (1992b) for rabbit SGLT1. k^0_{16}, k^0_{61}, k^0_{25}, k^0_{52}, k^0_{34}, k^0_{43}, k^0_{45}, k^0_{56}, k^0_{32}, and k^0_{21} are expressed in s^{-1}; k^0_{23} and k^0_{54} are expressed in $s^{-1}mol^{-1}$; k^0_{12} and k^0_{65} are expressed in $s^{-1}mol^{-2}$. $u = FV_m/RT$, where F, R, and T have their usual meanings. (*B*) Numerical comparison of inward Na leak ($J_{2\to5}$) and inward Na-αMG cotransport ($J_{3\to4}$) as a function of external αMG concentration using the model parameters given in *A*. The dotted line represents the ratio between the two forms of Na influx. The αMG_o concentration at which the two curves intersect is K_c (= 32 μM). The inset is a depiction at low $[\alpha MG]_o$.

of the cotransport flux and the Na leak can be easily discerned at any $[\alpha MG]_o$. In this simulation, $[Na]_o$ = 100 mM, $[Na]_i$ = 15 mM, $[\alpha MG]_i$ = 0, V_m = −100 mV, temperature = 22°C, and each oocyte is assumed to contain 10^{11} cotransporters.

In summary, we have analyzed the coupling between Na and glucose fluxes through the human SGLT1 protein. In intact oocytes, the relationship between external αMG concentrations and reversal potentials has indicated a stoichiometry close to two Na ions per glucose molecule and demonstrated that the Na leak represents a significant proportion of SGLT1 transport whenever $[\alpha MG]_o$ is close to or below a newly defined parameter K_c (K_c = 40 ± 12 μM). Using internally perfused oocytes, the 2:1 stoichiometry has been confirmed with considerable accuracy, and a "pure" Na leak was directly observed in the bilateral absence of glucose. This leak current was shown to present strong inward rectification, indicating significant asymmetries in the transport mechanism. It will be interesting to apply these procedures to examine the Na leak and coupling stoichiometry associated with expression of a purported SGLT regulatory subunit RS1 (Veyhl et al., 1993) as well as the recently identified SGLT2 transporter (Mackenzie et al., 1994).

APPENDIX

The generalized ordered kinetic model with mirror symmetry is illustrated in Fig. 2 *A*. On the external side of the oocyte, *n* Na ions bind to a free carrier C (state 1) through an arbitrary number of steps to form a complex CNa_n (state 2), then one glucose molecule binds to CNa_n to yield CNa_nG (state 3). The situation for the internal side is symmetrical to the external side. Transition 1 ↔ 6 (3 ↔ 4) represents a free (fully loaded) carrier translocation across the membrane, and 2 ↔ 5 represents the Na leak. In the model, we assume that the free carrier possesses *n* elementary negative charges, so that transitions 2 ↔ 3, 3 ↔ 4, 4 ↔ 5, and 5 ↔ 2 are independent of the membrane potential. Let k_{ij} be k^0_{ij} multiplied by the corresponding voltage dependence factor and substrate concentration; then steady-state transmembrane current can be calculated as follows:

$$I = nFN_T(k_{16}C_1 - k_{61}C_6) \tag{A1}$$

where C_i represents the probability of finding a carrier in the state *i*, N_T is the total number of carriers in moles, and *F* is the Faraday constant.

Occupation probabilities (C_i) can be calculated based on the schematic method of King and Altman (1956). By inspecting all patterns, only four were found to give non-zero contributions to the transmembrane current. These four patterns are shown in Fig. 2 *B*. Let $k_{i\to j}$ be the product of the rate constants of all transitions from state *i*, through intermediate states inside the box, to state *j* (Fig. 2 *A*). Then the four patterns contribute to the current (Eq. A1), respectively, in accordance with the following four expressions:

$$\begin{aligned}
&k_{16}k_{6\to5}k_{54}k_{43}k_{32}k_{2\to1} - k_{61}k_{1\to2}k_{23}k_{34}k_{45}k_{5\to6}\\
&k_{16}k_{6\to5}k_{52}k_{32}k_{45}k_{2\to1} - k_{61}k_{1\to2}k_{25}k_{32}k_{45}k_{5\to6}\\
&k_{16}k_{6\to5}k_{52}k_{43}k_{32}k_{2\to1} - k_{61}k_{1\to2}k_{25}k_{43}k_{32}k_{5\to6}\\
&k_{16}k_{6\to5}k_{52}k_{34}k_{45}k_{2\to1} - k_{61}k_{1\to2}k_{25}k_{34}k_{45}k_{5\to6}.
\end{aligned} \tag{A2}$$

Using the following two microscopic reversibility relations

$$k^0_{16}k^0_{6\to5}k^0_{54}k^0_{43}k^0_{32}k^0_{2\to1} = k^0_{61}k^0_{1\to2}k^0_{23}k^0_{34}k^0_{45}k^0_{5\to6}$$

and

$$k^0_{52}k^0_{23}k^0_{34}k^0_{45} = k^0_{54}k^0_{43}k^0_{32}k^0_{25},$$

the first expression in (A2) can be written as

$$k^0_{cycle}([G]_i[Na]_i^n e^{nFV/2RT} - [G]_o[Na]_o^n e^{-nFV/2RT}), \tag{A3}$$

and the sum of the other three expressions can be written as

$$k^0_{cycle}K_c([Na]_i^n e^{nFV/2RT} - [Na]_o^n e^{-nFV/2RT}), \tag{A4}$$

where $k^0_{cycle} = k^0_{61}k^0_{1\to2}k^0_{23}k^0_{34}k^0_{45}k^0_{5\to6}$, and K_c is a characteristic concentration constant and a function of the rate constants linking states 2, 3, 4, and 5 to each other:

$$K_c = \frac{k^0_{25}(k^0_{32}k^0_{45} + k^0_{43}k^0_{32} + k^0_{34}k^0_{45})}{k^0_{23}k^0_{34}k^0_{45}} = \frac{k_{25}(k_{32}k_{45} + k_{43}k_{32} + k_{34}k_{45})}{k_{23}k_{34}k_{45}}. \quad \text{(A5)}$$

The current in Eq. A1 is simply the sum of expressions (A3) and (A4) divided by ΣS_i, the sum of the King-Altman patterns for all states, yielding

$$I = \frac{nFN_Tk^0_{cycle}}{\Sigma S_i}[([G]_i + K_c)[Na]^n_i e^{nFV/2RT} - ([G]_o + K_c)[Na]^n_o e^{-nFV/2RT}]. \quad \text{(A6)}$$

Then the following relationship between V_r and substrate concentrations can be obtained under the zero current conditions:

$$V_r = \frac{RT}{nF}\ln\frac{([G]_o + K_c)[Na]^n_o}{([G]_i + K_c)[Na]^n_i}. \quad \text{(A7)}$$

The meaning of K_c can be illustrated from the expressions for the net fluxes J_{25} and J_{34}:

$$J_{25} = N_T(k_{25}C_2 - k_{52}C_5)$$

$$J_{34} = N_T(k_{34}C_3 - k_{43}C_4) = N_T(k_{25}C_2[G]_o - k_{52}C_5[G]_i)/K_c. \quad \text{(A8)}$$

Equation A8 can be derived because C_3 and C_4 can be expressed as functions of C_2 and C_5 using the following steady-state conditions:

$$(k_{34} + k_{32})C_3 = k_{43}C_4 + k_{23}C_2$$
$$(k_{43} + k_{45})C_4 = k_{34}C_3 + k_{54}C_5. \quad \text{(A9)}$$

In the case where the transitions between states 2 and 5 are much slower than the binding to and debinding from the carrier, $N_Tk_{25}C_2$ and $N_Tk_{52}C_5$ represent, respectively, the inward and outward Na leaks. It can be seen from Eq. A8 that K_c corresponds to the extracellular sugar concentration for which the inward Na leak ($N_Tk_{25}C_2$) is equal to the coupled Na-sugar influx ($N_Tk_{25}C_2[G]_o/K_c$). A similar conclusion can be made with regard to intracellular sugar concentration and outward Na and Na-sugar fluxes. In addition, if $[G]_i = [G]_o$, K_c corresponds to the sugar concentration for which the net Na leak equals the net Na-sugar cotransport.

Thanks to Ms. Bernadette Walendorff and Mathilde Cartier for excellent technical assistance.

This work is supported by the Medical Research Council of Canada (grant 16580 awarded to J.Y.L.), and the cloning of SGLT1 is supported by a grant from the Kidney Foundation of Canada awarded to A.B.

REFERENCES

Coady, M. J., F. Jalal, X.-Z. Chen, G. Lemay, A. Berteloot, and J.-Y. Lapointe. 1994. Electrogenic amino acid exchange via the rBAT transporter. *FEBS Lett.* 356:174–178.

Costa, A. C. S., J. W. Patrick, and J. A. Dani. 1994. Improved technique for studying ion channels expressed in *Xenopus* oocytes, including fast superfusion. *Biophys. J.* 67:395–401.

Crane, R. K. 1977. The gradient hypothesis and other models of carrier mediated active transport. *Rev. Physiol. Biochem. Pharmacol.* 78: 99–159.

Dascal, N. 1987. The use of *Xenopus* oocytes for the study of ion channels. *CRC Crit. Rev. Biochem.* 22:317–387.

Hediger, M. A., M. J. Coady, T. S. Ikeda, and E. M. Wright. 1987. Expression cloning and cDNA sequencing of the Na^+/glucose cotransporter. *Nature.* 330:379–381.

Hediger, M. A., E. Turk, and E. M. Wright. 1989. Homology of the human intestinal Na^+/glucose and *E. coli* Na/proline cotransporters. *Proc. Natl. Acad. Sci. USA.* 86:5748–5752.

Huang, H., H. St.-Jean, M. J. Coady, and J.-Y. Lapointe. 1995. Evidence for coupling between Na^+ pump activity and TEA-sensitive K^+ currents in *Xenopus laevis* oocytes. *J. Membr. Biol.* 143:29–35.

Kaluz, S., K. Kölble, and K. B. M. Reid. 1992. Directional cloning of PCR products using exonuclease III. *Nucleic Acids Res.* 20:4369–4370.

Kessler, M., and G. Semenza. 1983. The small intestinal Na^+, D-glucose cotransporter: an asymmetric gated channel (or pore) responsive to V_m. *J. Membr. Biol.* 76:27–56.

Kimmich, G. A. 1990. Membrane potential and the mechanism of intestinal Na^+-dependent sugar transport. *J. Membr. Biol.* 114:1–27.

Kimmich, G. A., and J. Randles. 1980. Evidence for an intestinal Na^+: sugar transport coupling stoichiometry of 2.0. *Biochim. Biophys. Acta.* 596:439–444.

Kimmich, G. A., and J. Randles. 1984. Sodium-sugar coupling stoichiometry in chick intestinal cells. *Am. J. Physiol.* 247:C74–C82.

King, E. L., and C. Altman. 1956. A schematic method of deriving the rate laws for enzyme-catalyzed reactions. *J. Phys. Chem.* 60: 1375–1378.

Lafaire, A. V., and W. Schwartz. 1986. Voltage dependence of the rheogenic Na^+/K^+ ATPase in the membrane of oocytes of *Xenopus laevis*. *J. Membr. Biol.* 91:43–51.

Lapointe, J.-Y., R. L. Hudson, and S. G. Schultz. 1986. Current-voltage relations of sodium-coupled sugar transport across the apical membrane of *Necturus* small intestine. *J. Membr. Biol.* 93:205–219.

Lee, W. S., Y. Kanai, R. G. Wells, and M. A. Hediger. 1994. The high affinity Na^+/glucose cotransporter. *J. Biol. Chem.* 269:12032–12039.

Lever, J. E. 1982. Expression of a differentiated transport in apical membrane vesicles isolated from an established kidney epithelial cell line. *J. Biol. Chem.* 257:8680–8686.

Loo, D. D. F., A. Hazama, S. Supplisson, E. Turk, and E. M. Wright. 1993. Relaxation kinetics of the Na^+/glucose cotransporter. *Proc. Natl. Acad. Sci. USA.* 90:5767–5771.

Mackenzie, B., M. P. Heiermann, D. D. F. Loo, J. E. Lever, and E. M. Wright. 1994. SAAT1 is a low affinity Na^+/glucose cotransporter and not an amino acid transporter. *J. Biol. Chem.* 269:22488–22491.

Mackenzie, B., D. D. F. Loo, and E. M. Wright. 1995. Direct determination of Na^+/glucose coupling stoichiometry for SGLT1 expressed in *Xenopus* oocytes. *FASEB J.* 9(part I):A260.

Moran, A., K. S. Handler, and R. J. Turner. 1982. Na^+-dependent hexose transport in vesicles from cultured renal epithelial cell line. *Am. J. Physiol.* 243:C293–C298.

Parent, L., S. Supplisson, D. D. F. Loo, and E. M. Wright. 1992a. Electrogenic properties of the cloned Na^+/glucose cotransporter. I. Voltage-clamp studies. *J. Membr. Biol.* 125:49–62.

Parent, L., S. Supplisson, D. D. F. Loo, and E. M. Wright. 1992b. Electrogenic properties of the cloned Na^+/glucose cotransporter. II. A transport model under nonrapid equilibrium conditions. *J. Membr. Biol.* 125:63–79.

Restrepo, D., and G. A. Kimmich. 1985. Kinetic analysis of mechanism of intestinal Na^+-dependent sugar transport. *Am. J. Physiol.* 248: C498–C509.

Restrepo, D., and G. A. Kimmich. 1986. Phlorizin binding to isolated enterocytes: membrane potential and sodium dependence. *J. Membr. Biol.* 89:269–280.

Schultz, S. G. 1980. The electrochemical potential. *In* Basic Principles of Membrane Transport. F. Hutchinson, W. Fuller, and L. J. Mullins, editors. Cambridge University Press, Cambridge. 8–13.

Scriver, C. R., and H. S. Tenenhouse. 1985. Genetics and mammalian transport systems. *Ann. N.Y. Acad. Sci.* 456:384–397.

Semenza, G., M. Kessler, M. Hosang, J. Weber, and U. Schmidt. 1984. Biochemistry of the Na^+, D-glucose cotransporter of the small intestinal brush-border membrane. *Biochim. Biophys. Acta.* 779:343–379.

Silverman, M. 1991. Structure and function of hexose transporters. *Annu. Rev. Biochem.* 60:757–794.

Smith-Maxwell, C., E. Bennett, J. Randles, and G. A. Kimmich. 1990. Whole cell recording of sugar-induced currents in LLC-PK_1 cells. *Am. J. Physiol.* 258:C234–C242.

Stevens, B. R. 1992. Vertebrate intestine apical membrane mechanisms of organic nutrient transport. *Am. J. Physiol.* 263:R458–R46.

Swick, A. G., M. Janicot, T. Cheneval-Kastelic, J. C. McLenithan, and M. D. Lane. 1992. Promoter-cDNA-directed heterologous protein expression in *Xenopus laevis* oocytes. *Proc. Natl. Acad. Sci. USA.* 89: 1812–1816.

Taglialatela, M., L. Toro, and E. Stefani. 1992. Novel voltage clamp to record small, fast currents from ion channels expressed in *Xenopus* oocytes. *Biophys. J.* 61:78–82.

Tate, S. S., R. Urade, L. Gerber, and S. Udenfriend. 1990. Secreted alkaline phosphatase: an internal standard for expression of injected mRNA in the *Xenopus* oocyte. *FASEB J.* 4:227–231.

Turner, R. J., and A. Moran. 1982a. Stoichiometric studies of the renal outer cortical brush border membrane D-glucose transporter. *J. Membr. Biol.* 67:73–80.

Turner, R. J., and A. Moran. 1982b. Further studies of proximal tubular brush border membrane D-glucose transport heterogeneity. *J. Membr. Biol.* 70:37–45.

Umbach, J. A., M. J. Coady, and E. M. Wright. 1990. The intestinal Na^+/glucose cotransporter expressed in *Xenopus* oocytes is electrogenic. *Biophys. J.* 57:1217–1224.

Veyhl, M., J. Spangenberg, B. Büschel, R. Poppe, C. Dekel, G. Fritzsch, W. Haase, and H. Koepsell. 1993. Cloning of a membrane-associated protein which modifies activity and properties of the Na^+-D-glucose cotransporter. *J. Biol. Chem.* 268:25041–25053.

Wright, E. M. 1993. The intestinal Na^+/glucose cotransporter. *Annu. Rev. Physiol.* 55:575–589.